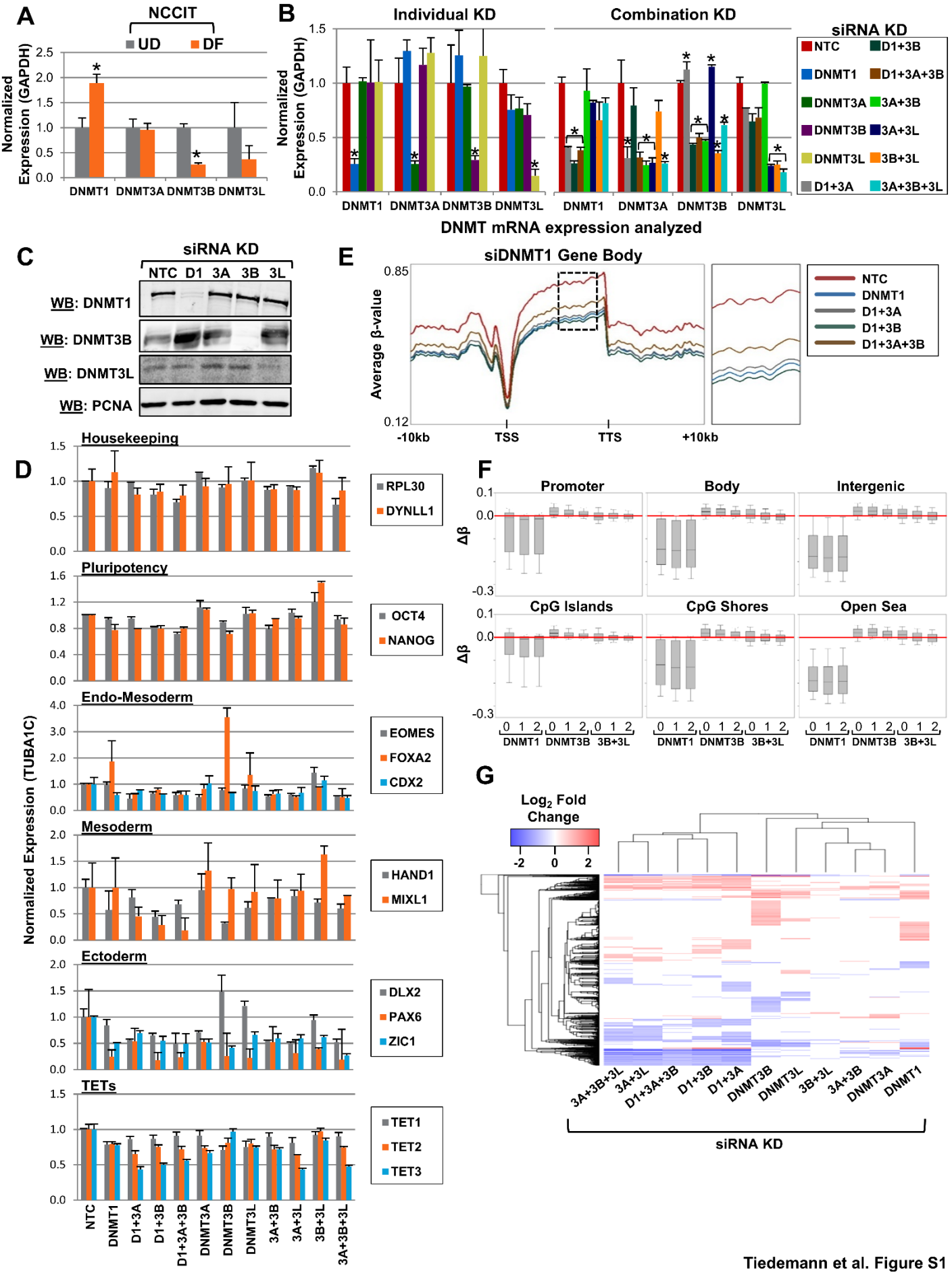

Tiedemann et al. Figure S1

A

	Hypomethylation		Hypermethylation	
Sample	#CpG	#Genes	#CpG	#Genes
DNMT1	286257	20641	144	119
D1+3A	256265	20281	53	39
D1+3B	264199	20460	50	44
D1+3A+3B	215529	19808	176	144
DNMT3A	130	98	145	103
DNMT3B	71	57	321	247
DNMT3L	29	18	57	45
3A+3B	43	28	207	154
3A+3L	64	50	67	55
3B+3L	105	81	411	290
3A+3B+3L	230	183	405	280

B

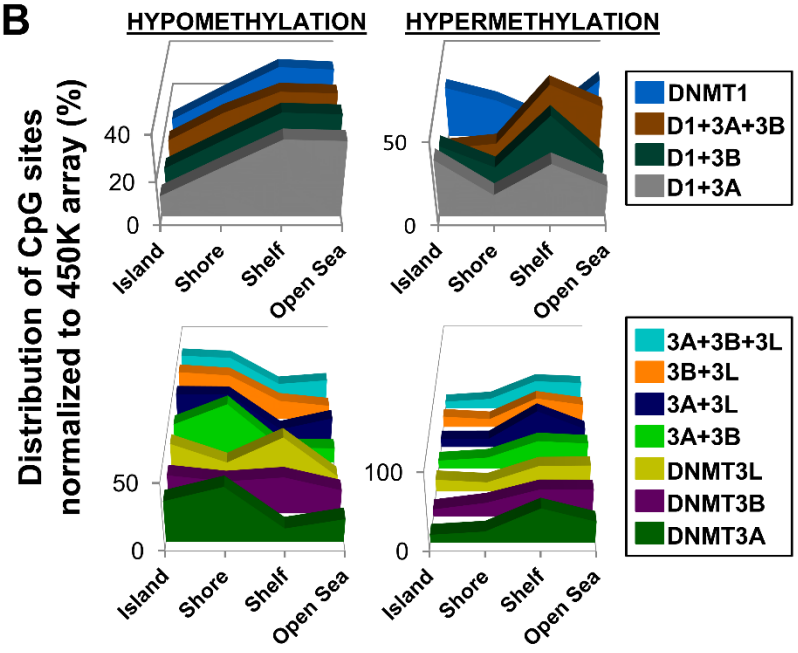

C

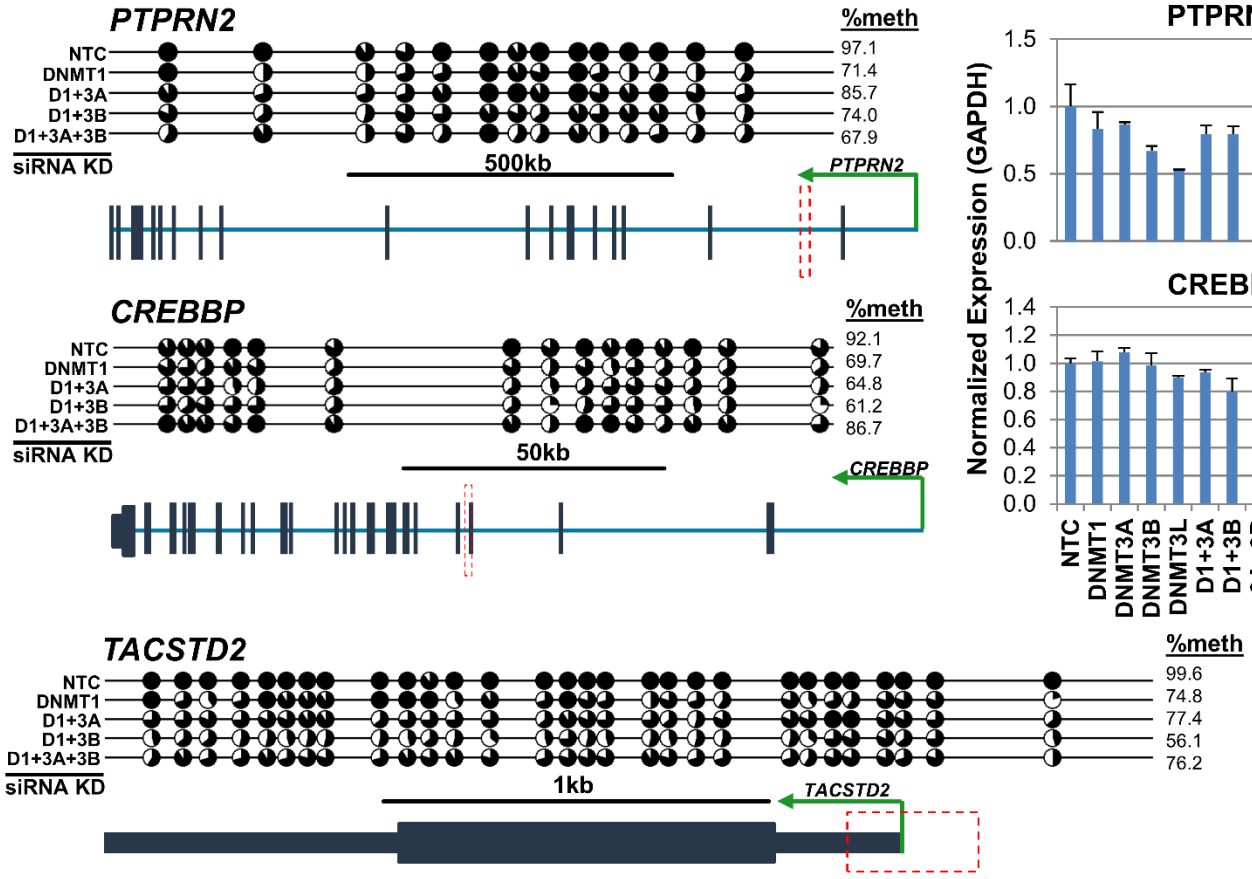

D

Tiedemann et al. Figure S2

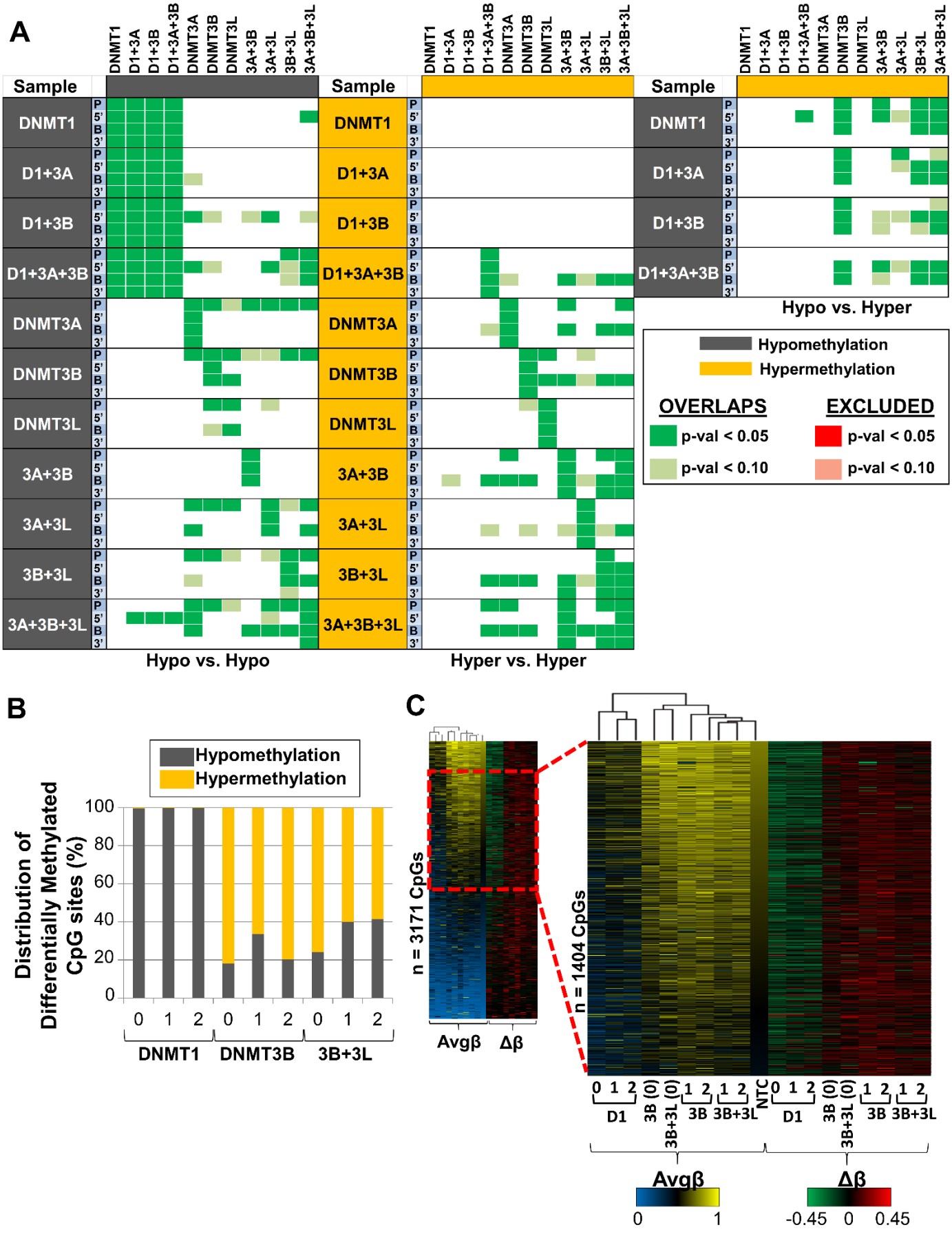

Tiedemann et al. Figure S3

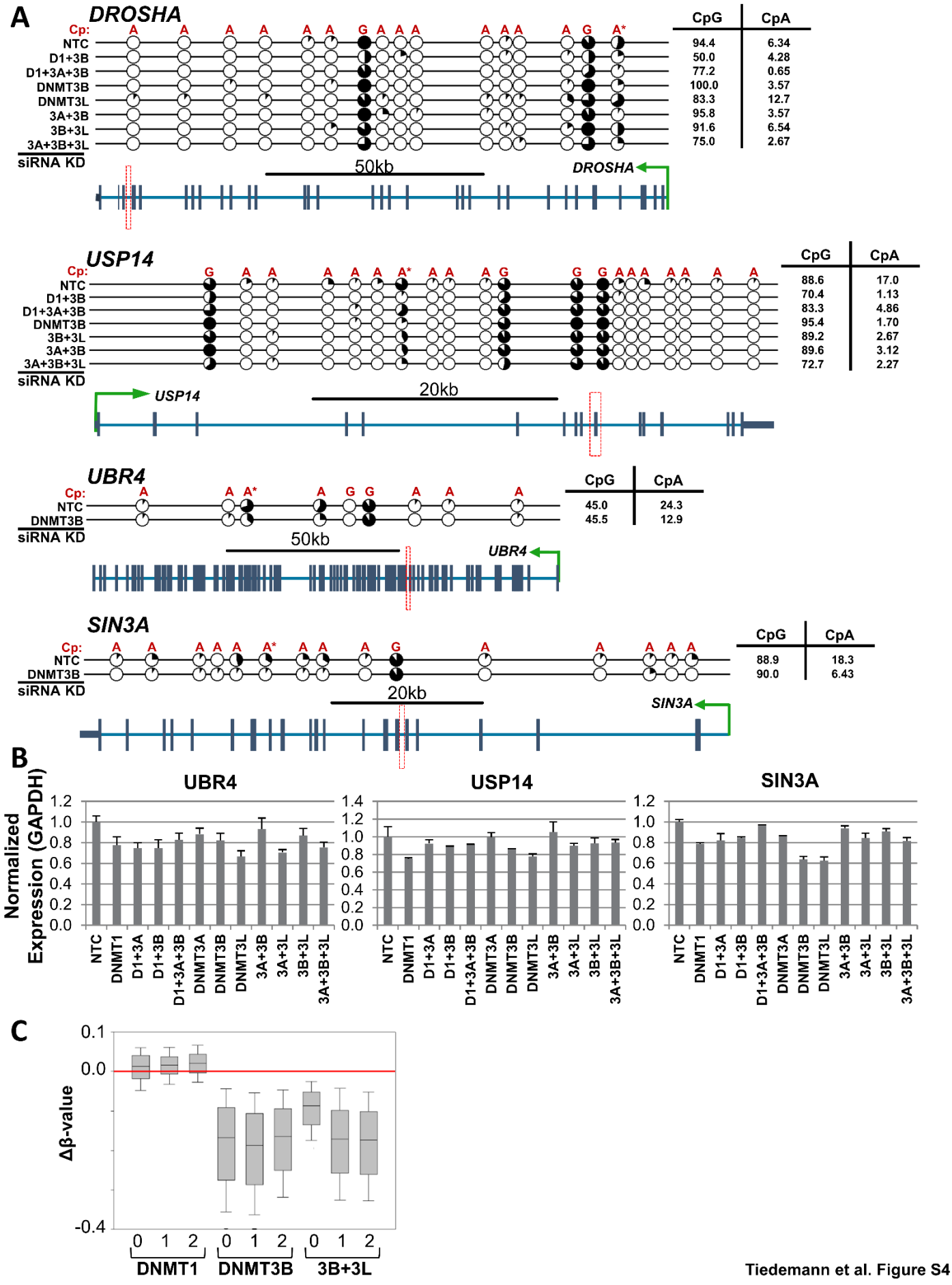

Tiedemann et al. Figure S4

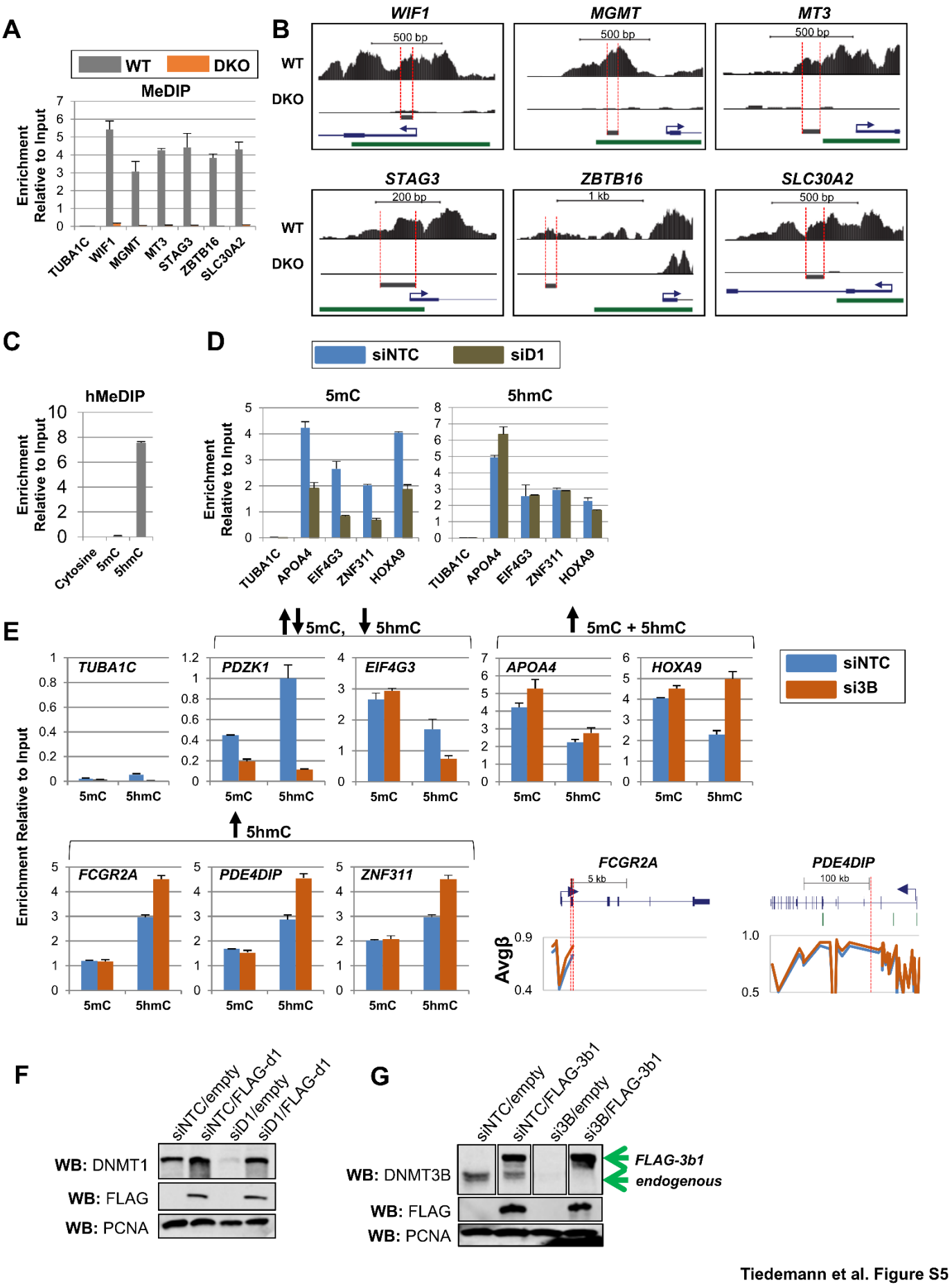

Tiedemann et al. Figure S5

A

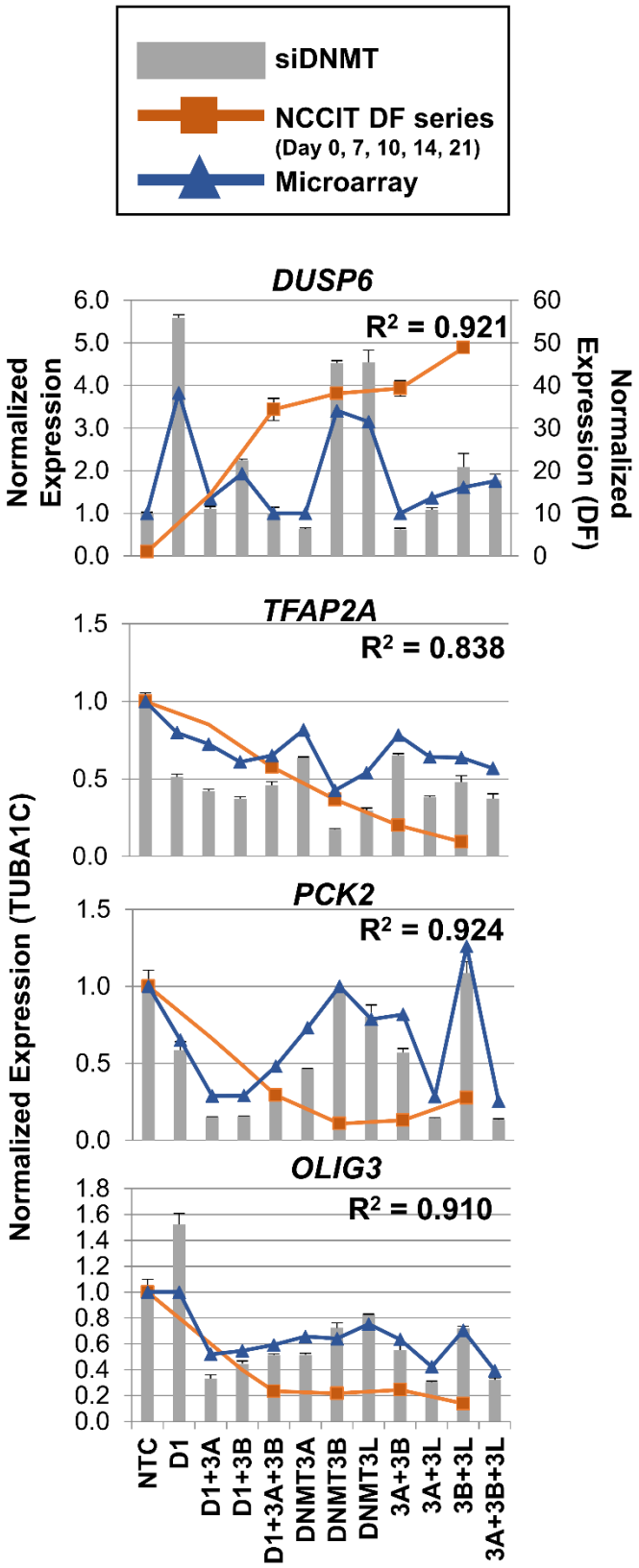

B

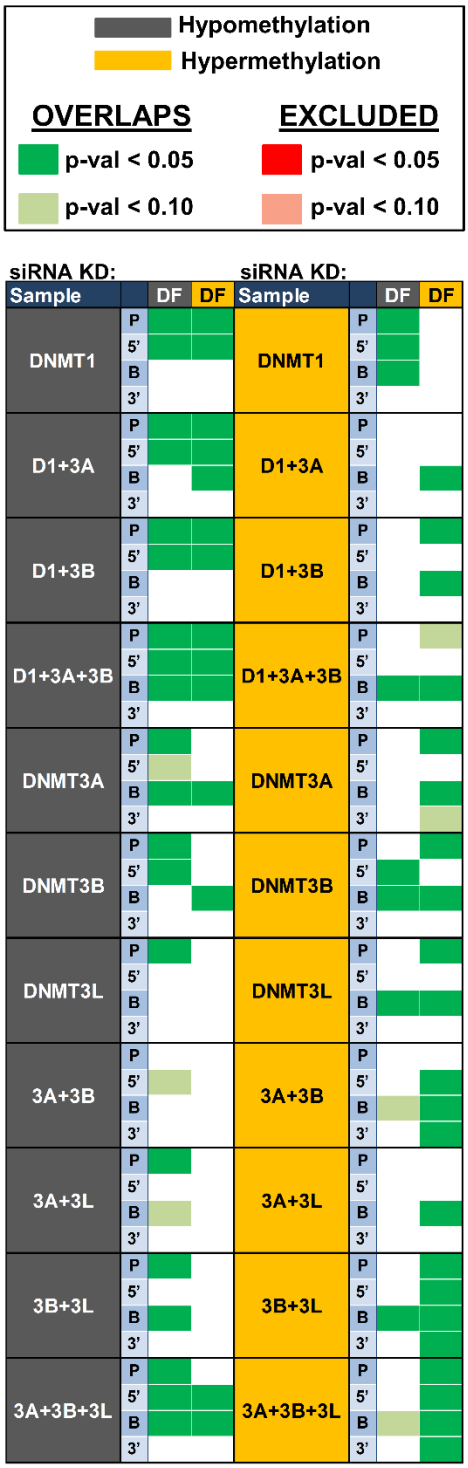

Tiedemann et al. Figure S6

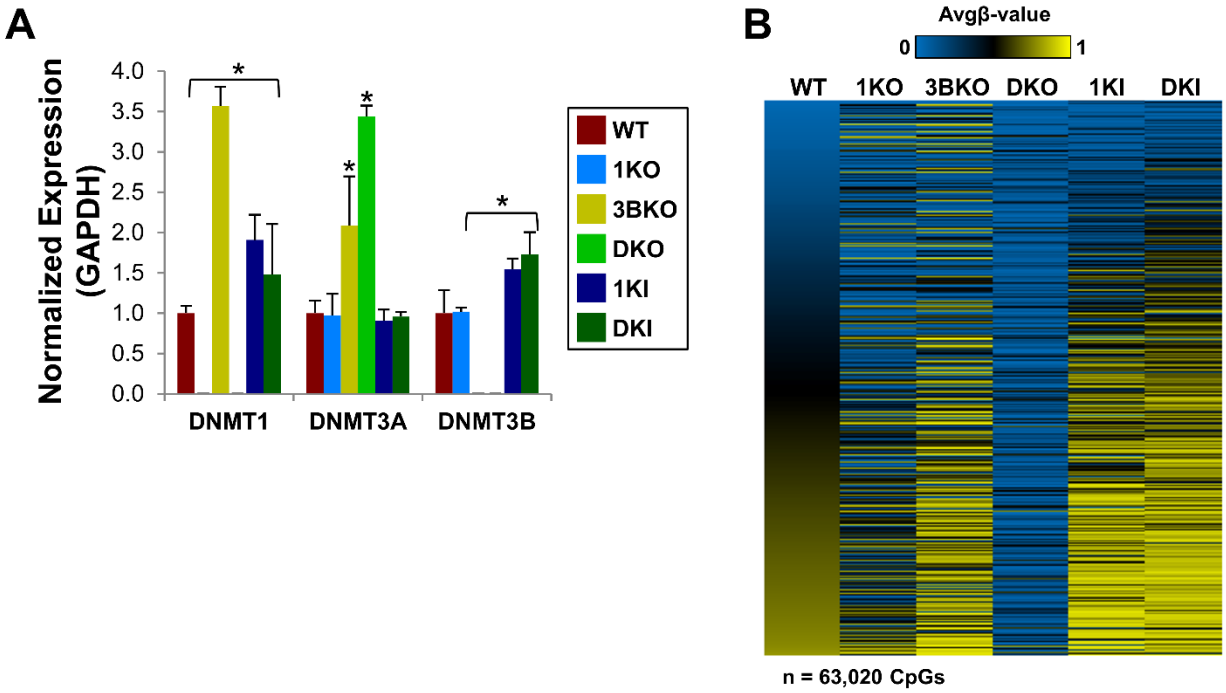

Tiedemann et al. Figure S7

SUPPLEMENTAL FIGURE LEGENDS

Figure S1. Validation of the experimental system used for this study, related to Figure 1. (**A**) mRNA expression by quantitative RT-PCR of DNMTs in undifferentiated (UD) and differentiated (DF) NCCIT cells performed in triplicate relative to GAPDH expression and normalized to UD (set at 1.0). Error bars indicate standard error. NCCIT UD cells were treated with retinoic acid (10μM) for 7 days prior to the RNA harvest for DF cells, and this represented the "differentiated" condition used throughout this study. ***** = pval < 0.005 (**B**) Expression of DNMTs in all DNMT siRNA knockdown (KD) samples (single and combination) by quantitative RT-PCR relative to GAPDH expression, normalized to a no-target control (NTC) siRNA transfection. Depletion efficiency was monitored on the same samples used for the HumanMethylation 450K and Affymetrix Gene 1.0 ST arrays. ***** = pval < 0.005. (**C**) Expression of DNMTs for individual NCCIT siDNMT KD samples at the protein level confirms the RT-PCR results. PCNA was used as a loading control. (**D**) Expression of developmental markers, pluripotency factors, housekeeping genes, and TETs by quantitative RT-PCR under conditions of DNMT depletion relative to TUBA1C expression, normalized to NTC. (**E**) Intragenic spatial distribution plot for DNMT1 siRNA depleted samples derived from average β-values for DNA methylation obtained from the HumanMethylation 450K array. TSS = transcription start site; TTS = transcription termination site. Dashed black box indicates region magnified (to the right) to better visualize relative methylation levels among samples. (**F**) Feature-based analysis of differential methylation demonstrates reproducibility among independent siDNMT KD biological replicates. Box plots representing all ∆β-values for each sample in the indicated genomic features (promoter, gene body, intergenic, islands, shores, open sea) in three independent KD experiments ("0, 1, 2"; 0 = original experiment). Outliers outside of the 5^{th}/95^{th} percentile have been removed. Red bar highlights the zero line (no change in methylation). (**G**) Clustered heat

map of gene expression (Affymetrix Human Gene 1.0 ST array) measured as $\log_2$ fold change for all NCCIT DNMT KD samples.

Figure S2. Confirmation of array-based CpG methylation data using bisulfite genomic sequencing, related to Figure 2. (**A**) Table showing numbers of hypo/hypermethylated CpG sites (including intergenic sites) and genes for each NCCIT siRNA DNMT depletion condition. (**B**) Normalized distribution of significantly differentially methylated CpG sites by CpG island annotation. Normalization was conducted by comparing the number of significantly differentially methylated CpG sites to the total number of sites for each island annotation present on the 450K array. **Top:** DNMT1 depletion (individual/combination) **Bottom:** DNMT3 depletion (individual/combination). (**C**) Bisulfite genomic sequencing (BGS) of identified DNMT1 target genes from the 450K array analysis. Gene structures with PCR-amplified region indicated by a dashed red box are provided below each CpG plot. Each pie chart indicates the percentage of methylated (black) and unmethylated (white) CpGs for a single CpG site among > 10 clones sequenced with the total percent methylation shown at the right. (**D**) Expression of PTPRN2 and CREBBP (DNMT1 target genes) by quantitative RT-PCR for all DNMT depleted samples relative to GAPDH expression, normalized to NTC. Error bars indicate standard error.

Figure S3. Overlap of significantly differentially methylated genes across all NCCIT DNMT siRNA depleted samples, related to Figure 2 (**A**) Overlap analysis of hypo/hypermethylated genes with significantly differentially methylated CpG sites (pval < 0.05) among genomic features (P = promoter, 5' = 5'UTR, B = body, 3' = 3'UTR) for all NCCIT DNMT depleted samples. Statistical significance of overlap was calculated using the Fisher's Exact test. **Left:** hypomethylation vs hypomethylation; **Middle:** hypermethylation vs hypermethylation; **Right:** siDNMT1 (single/combo) hypomethylation vs hypermethylation. For example, in the right panel, genes that become hypomethylated in the gene body of DNMT1 depleted samples significantly overlap with genes that become hypermethylated in the gene body upon DNMT3B individual

and combination siRNA depletion. (**B**) Distribution of differentially methylated CpG sites for siDNMT KD biological replicates**.** Percentage of significantly differentially methylated CpG sites (pval < 0.05) classified by methylation status (hypo/hypermethylation) in three independent NCCIT DNMT depletion experiments demonstrates the reproducibility of our findings. (**C**) Clustered heat map of hypermethylated CpG sites for each DNMT depleted biological replicate sample to demonstrate reproducibility of the siDNMT3B hypermethylation phenotype at conserved loci. Hypermethylated (Δβ>0.15) CpG loci (duplicate CpG sites removed) were clustered by siDNMT samples stratified by NTC most methylated CpG sites to least methylated CpG sites (left panel). Δβ-values for respective CpG loci are also presented (right panel). Dashed red box indicates magnified region (Avgβ-value [0.45 – 0.75] in NTC).

Figure S4. Independent confirmation of array-based nonCpG methylation data using bisulfite genomic sequencing, related to Figure 3. (**A**) Bisulfite genomic sequencing (BGS) analysis of nonCpG hypomethylation events in DNMT3 depleted samples identified using the 450K array data. CpH status is indicated above each BGS plot; the 450K array CpA is denoted by *****. Gene structures with amplified region indicated by the dashed red box provided below each CpH plot. Each pie chart indicates the percent methylated (black) and unmethylated (white) CpHs for a single CpH site among at least 10 clones sequenced. The table to the right of each plot indicates the total percent methylation for all CpGs and CpAs shown in each sample. (**B**) Expression of UBR4, USP14, and SIN3A by quantitative RT-PCR for all DNMT depleted samples relative to GAPDH expression, normalized to NTC. Error bars indicate standard error. (**C**) Box plots of Δβ-values for nonCpG methylation among three independent, biological replicates of siDNMT1, siDNMT3B, and si3B+3L conditions (“0, 1, 2”; 0 = original experiment). Outliers outside of the 5^{th}/95^{th} percentile have been removed. Red bar highlights the zero line (no change in methylation).

Figure S5. Independent confirmation of array-based CpG methylation and TAB-seq results using MeDIP/hMeDIP pull-downs, related to Figure 4. (**A**) **Validation of MeDIP technique.** HCT116 colorectal carcinoma (WT) and DNMT1/DNMT3B knockout (DKO) cells were assayed for 5mC at promoters of selected genes with previously established changes in 5mC levels (selected based on the MBD-seq method – data not shown) by pull-down with the Diagenode 33D3 5mC antibody. WT cells demonstrate enrichment for 5mC while DKO cells show no enrichment for 5mC at these loci. TUBA1C serves as an unmethylated control and is not enriched in either cell line. (**B**) **Representative browser shots demonstrating 5mC profiles for HCT116 WT and DKO cells.** Confirmed utility and specificity of the MeDIP technique for 5mC by assaying promoters predicted to have methylation from MBD-seq analysis of HCT116 WT and DKO cells (unpublished data). Red lines indicate the MeDIP PCR amplification region. Green bars represent CpG islands. (**C**) **Validation of in-house produced 5hmC antibody by spike-in hMeDIP.** HCT116 WT DNA was spiked with unmodified (Cytosine), methylated (5mC), and hydroxymethylated (5hmC) controls (Diagenode). hMeDIP was performed using the same protocol as for MeDIP, and enrichment for spike-in controls was analyzed by qPCR in triplicate reactions. The 5hmC antibody demonstrated specific enrichment of the hydroxymethylated control sequence, but not the methylated and unmethylated sequences. (**D**) **MeDIP/hMeDIP analysis of siDNMT1 target loci.** siRNA depletion of DNMT1 in NCCIT cells followed by (h)MeDIP revealed reduced enrichment for 5mC across all assayed regions relative to NTC. 5hmC enrichment was locus-specific with the assayed regions demonstrating small gains (*APOA4*), loss (*HOXA9*), or no change (*ZNF311, EIF4G3*) in 5hmC. (**E**) **MeDIP/hMeDIP analysis of siDNMT3B target loci.** 5mC and 5hmC in NCCIT cells depleted for DNMT3B was locus dependent but consistent with 450K array/MBD-seq-based data. *PDZK1* and *EIF4G3* (identified from MBD-seq, browser shots in main text Fig. 6D) resulted in loss (*PDZK1*) and gain (*EIF4G3*) of 5mC, consistent with MBD-seq results; 5hmC

was reduced at these loci. The *FCGR2A*, *PDE4DIP*, and *ZNF311* loci showed consistent 5mC levels, while 5hmC levels increased in DNMT3B depleted cells. The *APOA4* and *HOXA9* loci showed elevated enrichment of both 5mC and 5hmC (note the *HOXA9* results are consistent with BGS/TAB-sequencing in Figure 4A). Gene structures showing (h)MeDIP assayed regions (red bars) in the *FCGR2A* and *PDE4DIP* loci are shown at the right (for other genes, refer to Figure 4C,D). β-values for CpG sites in these two loci that are present on the 450K array (scaled to length of the gene) are presented in graphical form below each gene schematic.

Supporting data validating the siRNA rescue experiment for (F) DNMT1 and (G) DNMT3B. (**F**) Western blot analysis of protein expression demonstrates efficient depletion of endogenous DNMT1 in the presence of transfected empty ectopic expression vector (empty) and efficient ectopic expression of FLAG-Dnmt1 at levels near that of endogenous DNMT1 in NCCIT cells transfected with the latter expression vector. (**G**) Western blot analysis of protein expression demonstrates efficient depletion of endogenous DNMT3B in the presence of transfected empty ectopic expression vector and efficient expression of FLAG-Dnmt3b1 at levels near that of endogenous DNMT3B in NCCIT cells transfected with the latter expression vector. Note that the gel photo was cut to facilitate comparison with part F because samples were loaded in a different order.

Figure S6. DNMT siRNA depletion mirrors the regulation of gene expression and DNA methylation observed during differentiation, related to Figure 6. (**A**) **Validation of microarray expression data.** QRT-PCR-based validation of differentially expressed genes identified from microarray analysis (blue line) performed in triplicate relative to TUBA1C expression and normalized to the NTC (siDNMT samples). Error bars indicate the standard error. mRNA expression (qPCR) of each gene upon differentiation of NCCIT cells with retinoic acid treatment (orange line) is overlaid to demonstrate concordance of expression profiles between siDNMT and NCCIT DF samples. NCCIT UD cells were treated with retinoic acid

(10μM) for 7, 10, 14, and 21 days prior to RNA harvest for DF cells. Microarray fold changes (blue line) are overlaid upon the qRT-PCR results (gray bars) for siDNMT samples to demonstrate the consistency between qPCR and microarray data. R^2 = Spearman rank correlation between siDNMT qRT-PCR and microarray data. The secondary axis (right) for *DUSP6* refers to fold expression changes for the NCCIT DF series as the increase in expression becomes more substantial (relative to the siDNMT samples) as differentiation proceeds. (**B**) Overlap analysis of hypo/hypermethylated genes with significantly differentially methylated CpG sites (pval < 0.05) among genomic features (P = promoter, 5' = 5'UTR, B = body, 3' = 3'UTR) for all NCCIT DNMT depleted samples versus NCCIT DF significantly hypo/hypermethylated genes.

Figure S7. Validation of HCT116 DNMT1/DNMT3B knockout and overexpression experimental system, related to Figure 7. (**A**) Expression of DNMT mRNA by quantitative RT-PCR for all HCT116 samples relative to GAPDH expression, normalized to WT (parental HCT116 cells). Error bars indicate standard error. ***** = pval < 0.05. (**B**) Heat map of hypermethylated (Δβ > 0.15) CpG sites for each HCT116 sample (duplicate CpG sites removed) stratified by WT (parental HCT116 cells) least methylated to most methylated CpG sites.

Table S1, Related to Experimental Procedures for QRT-PCR, BGS, and MeDIP.

QRT-PCR	Forward primer	Reverse primer
GAPDH	CTTTGGTATCGTGGAAGGACTC	GTAGAGGCAGGGATGATGTTC
DNMT1	GGAGAGGCTAAGCGTTCAAG	AAATGAGATGTGATGGTGGTTTG
DNMT3A	AAGAGCACAGCGGAGAAG	GCAGATGTCCTCAATGTTCC
DNMT3B*	CCATGAAGGTTGGCGACAA	TGGCATCAATCATCACTGGATT
DNMT3L*	GGGACAACTGAAGCATGTGGT	AAGATCGAAGGGTCCCCACT
TUBA1C	CCGGGCAGTGTTTGTAGACTTGG	ATCTCCTTGCCAATGGTGTAGTGCC
DYNLL	CATAGAGAAGGACATTGCGGCTCATATC	GAACAGAAGAATGGCCACTTGGC
RPL30	TTGAACTGGGCACAGCATGCGG	CTTTTCACCAGTCTGTTCTGGCATGC
OCT4	CTTGCTGCAGAAGTGGGTGGAGGAA	CTGCAGTGTGGGTTTCGGGCA
NANOG	GAACTCTCCAACATCCTGAACC	TTCTGCGTCACACCATTGC
HAND1	AAAGGCTCAGGACCCAAGAA	CAGCACGTCCATCAGGTAGG
CDX2	GCTACATCACCATCCGGAG	GCTGCTGCAACTTCTTCTTG
DLX2	AGACTCAATACTTGGCCTTGC	GCGAAGCACAAGGTGGAGAAGCG
ZIC1	CAAGTCCTACACGCATCCCAG	CGTGGAGGATTCGTAGCCAGAG
FOXA2	TATGCTGGGAGCGGTGAAGATGG	CGTGTTCATGCCGTTCATCC
MIXL1	CAAGCGCACGTCTTTCAGC	GCACAGTGGTTGAGGATAATCT
PAX6	GCCCGGCCGTGCGACATTTCC	GCACTTGGACTTTTGCATCTGCATGGG
EOMES	GGCAAATGGGTGACCTGTG	GAAATCTCCTGTCTCATCC
TET1	GGGCACCCTACCGACAGAAGATGC	CTTCTGGGGCTTGGGCTTCTACC
TET2	GGATGTCCTATTGCTAAGTGG	GAATCACAATCACTGCAGCCTC
TET3	GAGCTGGCGGGCATTACG	TGCGGCTCCACCTTGAGG
PTPRN2	TTCACCTCTGGGAGATTCCGAAGACCCCTCCAG	AGGGCTGCCTCGAGCTACTCCATGG
CREBBP	ACAGAGCATGGTCAACAGTTTGCCCACCTTCC	CAGTGGGGCCTGTTGCAATTGCTTG
UBR4	GGAGTCTGTGGCAACTGTGGAGAGAATG	CCGGTCTTCTTCATTCTCAATGGGATCCACT
USP14	CGATCAGTTCTTCGGTGTTGAGTTTGAAACT	GGCATTTCTTTGCAACGTTGGAGACTGTTTGGTG
SIN3A	TTGACCAGGTGAAGCTGCAGTTTGGTAG	CCTTTGAATAGCTGGGACACACGACTAATC
DUSP6	AGAGCAGCAGCGACTGGAACGAGAATA	AGCCGTCTAGATTGGTCTCGCAAT
TFAP2A	CGGATAATATCAAGTACGAGGACTGCG	CTCGTGTAGGGAGATTGACCTACAGT
PCK2	GTGACTTTGTCAAGTGTCTGCACTCCG	GCACGTGGCCAATCAGGGTTTTCTCT
OLIG3	ATGGATGAGATGTACCTGAGGGACCA	CCGGGCATCTTCTGCATCATAT
BGS/TAB	**Forward primer**	**Reverse primer**

PTPRN2	GAAAAATAGATGAGGTAGTAATTGAGAGAT	TACCAAACCCTACCTTCTTAAAATCTA
CREBBP	AGTAGATAAGATTTTTTGGAGTATTTGAT	AAATACAAACATCAATAAAAATTATACCC
TACSTD2	TTTTATTGGTATTTGGGTGATATATTT	CTAATAATCCCTACCTATCAAAACTAAT
DROSHA	TTGAAGTAGAGTAATTATTTTGAGA	ACCTTAATTTCTCTTTAACAAAA
USP14	GTATGTTGAAATGAATTTTGGGAGATTAA	AACAACAATTCTAACATTCC
UBR4	GGTTAAAAAATGTTAATGTTAGGGG	AACCCCACAACAACTTCAAATTCT
SIN3A	TAGAAAAATGTTGTATGAAAATTT	CTTATACATAACCACCAACCACA
HOXA9	AAGGTAAGAAGTGGAAGGAAT	ACCTTATAACATTAAACCTAAAC
GPX6	GGAATTAGAATATGGTTATTTGG	TCTAACTATAACATCAACTCTAACT
(h)MeDIP	**Forward Primer**	**Reverse Primer**
TUBA1C	TCACTACTTCTCCCCCGGACT	CCCACTCACCATGACTAGAACTTG
WIF1	AGCCCTTCCCGCTCTTCTGTT	CGGCAGAGACGTAAGACTGGCAAA
MGMT	CGCTTTCAGGACCACTCG	CAAATGGCCCGTACCTTTTC
MT3	AGTCAGTGTCGGGCTCATCGTGA	CCTGCCTCTCTTCCCCTTCATTCT
STAG3	ATCAGCTCGCACACTTCCAAACCTC	AAAGATTCCAGAAAAGCGCGGGA
ZBTB16	GCATGGAGGTGTGATTCTAGGTGAGT	TCGAGGTCACGCGGTTTTAGCAAT
SLC30A2	CACAGCCCATTATCTTCGTTCCCTCA	ACCTCCGCATTTGCCATCCTAGCAGT
APOA4	TTGAGCTCCTCGGCGTTCTTCTT	ACGCCCTACGCTGACGAATTCA
EIF4G3	GTAGAGACGGGGTTTCACTGTGTTAGC	TATTAAAGGCTAGGCGTGGTGGC
ZNF311	TCTCTGATGGATGGTAAGGCAGTGC	GACTTCAGCATCAAGGCAGAACTCAC
HOXA9	GCGGATTTGAAGGGAGGAGACACTT	GACACTCACACTTTGTCCCTGACTGAC
PDZK1	AAGTGAGAATCCAGGGCAGAGGGAA	CCCCAAGGAGCAGTAGCCTATAA
FCGR2A	ATCAACGTGCTCCAGGAGGACT	TGTTGTTGGCCTTGAACCTGTAGCTGG
PDE4DIP	GGCGTGATGGTATGTTCTTGTAGTCC	GTCTTGCTCTGTCATCCAGACTTGAG

Table S1. Primer sequences for QRT-PCR and BGS-PCR, related to Experimental Procedures. *indicates primer sequences from Ehrlich *et al.* (Ehrlich et al., 2006).

SUPPLEMENTAL EXPERIMENTAL PROCEDURES

siRNA transfections

For siRNA transfections, 7.0 x 10^4 NCCIT cells were seeded into each well of a 6-well plate. At 24 and 48 hours post seeding, cells were transfected using PepMute siRNA transfection

reagent (SignaGen) prepared according to the manufacturer's protocol. Fresh growth medium (900 µl) was added to cells 30 minutes prior to addition of 100 µl of transfection reagent mix. The siRNA transfection mix was comprised of 100 µl of PepMute transfection buffer, 1.5 µl of PepMute reagent, and 40 nM of siRNA for individual (including NTC sample) and triple combination KDs; 20 nM for double combination KDs (differing concentrations of siRNA molecules to be transfected for double and triple DNMT KDs were determined after extensive optimization). Fresh media was added to cells at 72 hours post-seeding, and cells were harvested at 96 hours post-seeding. For the siRNA rescue experiments, siRNA transfections were performed exactly as described above, with the exception that 14.0 x 10^4 NCCIT cells were seeded into each well of a 6-well plate. For DNMT KD, a pool of four siRNAs was used to ensure depletion of all transcript variants. Rather than generate human DNMT1/DNMT3B cDNA resistant to all siRNAs, we used full-length murine Dnmt1/Dnmt3b1, which are 74/94% homologous at the amino acid level to human DNMT1/DNMT3B1, but are not susceptible to targeting by the human siRNAs at the mRNA level. FLAG-Dnmt1 (pCMV-MTase/f) (Zimmermann et al., 1997), FLAG-Dnmt3b1 (pCAG-FLAG-Dnmt3b1-IRES-puro) (Kashiwagi et al., 2011), and the respective empty vectors were transfected 12-hours after the initial siRNA transfection using X-tremeGENE HP (Roche) transfection reagent according to the manufacturer's protocol. Briefly, 3 µg of the vector DNA, 9 µl of X-tremeGENE HP reagent, and 200 ul Opti-MEM (Life Technologies) were combined and incubated at room temperature for 30 minutes. Transfection mixture (200 µl) was then added drop-wise to each well.

Western Blot

Nuclear protein extracts were resolved on a 10% SDS-PAGE gel, and transferred overnight to PVDF membrane (Immobilon-FL). LI-COR fluorescent secondary antibodies were used for detection. Antibodies (and dilutions): DNMT1 (in-house) N1020 rabbit IgG (1:2000); DNMT3B

Novus NB300-516 (1:1000); DNMT3L (in-house) 8226 rabbit IgG (1:250); PCNA (PC10) Santa Cruz sc-56 (1:1000); FLAG (F1804) Sigma-Aldrich (1:500).

450K array data analysis

Quality control of 450K array samples was assessed using the Genome Studio Methylation Module (Illumina). Subset-quantile Within Array Normalization (SWAN) was performed on IDAT files via the R Bioconductor package "minfi" (Maksimovic et al., 2012). Probes with a detection pval > 0.05 were eliminated from the analysis. Probes from the X and Y chromosome were retained for downstream analysis as both NCCIT and HCT116 cell lines are derived from males. Significant differential methylation was determined from GenomeStudio Methylation Module Illumina custom algorithm for calculating DiffScores (DiffScore ≤ -13.0 (≈ pval < 0.05) = hypomethylation; DiffScore ≥ 13.0 (≈ pval < 0.05) = hypermethylation). Spatial distribution plots for 450K array data were generated using in-house scripts. Normalization for the genomic feature enrichment plots was conducted by comparing the number of significantly differentially methylated CpG sites to the total number of sites in each genomic feature present on the 450K array. Clustered heatmaps were generated using R and custom macros in Microsoft Excel.

MBD-seq data analysis

Raw sequencing reads were mapped to the UCSC human genome hg19 build using BWA V0.5.9 (Li and Durbin, 2009) with a default parameter setting. Multiply mapped reads and uniquely mapped reads with mismatches and indels > 5% of read lengths were filtered out. SICER V1.1 (Zang et al., 2009) was used to identify peaks in a sample and differentially enriched regions between two samples relative to an input with the following parameters: redundancy allowed = 1, window size = 200, fragment size = 300, effective genome size = 0.833, gap size = 400, E-value = 1000, false discovery rate = 0.01. In-house scripts annotated peaks and differentially enriched regions with RefSeq, CGIs, and repeats in the UCSC genome browser (Fujita et al., 2011), and classified them as promoter (−1kbp - +1 for TSS), body, and 3′

end (TTS + 1kbp). In some cases, gene bodies were further classified into 5′ UTR, exon, protein coding exon, 3′ UTR, and intron. After discarding more than two reads mapping to the same location, mapped reads were lengthened to the 3′-end to reflect their original length, and counted based on their midpoint for genomic features such as genes, CGIs, and repeats. A genomic feature was binned by relative positions including upstream and downstream regions. Different numbers of mapped reads per sample were taken into account by calculating FPKM (fragments per kilobase per million fragments mapped). To illustrate the change in tag densities around genes, a relative length window for gene bodies was used and the average of normalized read coverage in a window was measured.

Gene ontology analysis and statistical methods for data set comparisons

Welch two-sample t-tests (unpaired, unequal variances) were conducted on β-values for each siRNA KD sample compared to the NTC for box plot significance analysis testing. Ontology analysis was performed using GO_BP and KEGG_pathway annotations within DAVID bioinformatics database applying a modified EASE score to the Fisher Exact test (Huang et al., 2008; Huang et al., 2009). The Fisher Exact test with a two-tailed pval calculation was used for testing the significance of data set comparisons as described previously for similar data sets (Widschwendter et al., 2007). For added stringency, a modified EASE score was applied to all Fisher Exact tests.

Bisulfite genomic sequencing and Tet-assisted bisulfite sequencing

BGS was performed as described (Van Emburgh and Robertson, 2011), and BGS plots were generated using QUMA (Kumaki et al., 2008). Tet-assisted bisulfite (TAB) conversion of DNA was performed using the 5hmC TAB-seq kit (Wisegene) as described (Yu et al., 2012), with minor modifications (Putiri et al., 2014). Subsequent bisulfite conversion, amplification, and sequencing was performed as previously described (Putiri et al., 2014). A minimum of 10 clones were sequenced for regular BGS, and a minimum of 15 clones were sequenced for TAB-seq.

Generation and characterization of 5-hydroxylmethylcytosine monoclonal antibody

Monoclonal 5-hydroxymethylcytosine (5-hmC) antibody (Clone hmc-5, IgG1k) was generated in the Mayo Clinic Antibody Hybridoma Core. Briefly, 5-hydroxymethyl cytidine (Berry & Associates, PY7596) was conjugated to BSA as described (Garro et al., 1968). The conjugate was injected into mice for immunization. Following the instruction from the methylated DNA standard kit (Active Motif), the 350-bp DNA substrates were amplified by PCR using 5-methylcytosine dNTP mix or 5-hydroxymethylcytosine dNTP mix (Zymo research). These DNA substrates were used to screen antibodies using dot blotting. The specificity of antibodies was further evaluated by dot blotting analysis using different amounts of DNA substrates. Finally, the 5hmC antibodies were tested using hMeDIP assays by spiking standards (5-hmC, 5-mC & cytosine DNA standard pack for hMeDIP (Diagenode)) into sheared HCT116 WT genomic DNA.

SUPPLEMENTAL EXPERIMENTAL REFERENCES

Ehrlich, M., Woods, C. B., Yu, M. C., Dubeau, L., Yang, F., Campan, M., Weisenberger, D. J., Long, T., Youn, B., Fiala, E. S., and Laird, P. W. (2006). Quantitative analysis of associations between DNA hypermethylation, hypomethylation, and DNMT RNA levels in ovarian tumors. Oncogene *25*, 2636-2645.

Fujita, P. A., Rhead, B., Zweig, A. S., Hinrichs, A. S., Karolchik, D., Cline, M. S., Goldman, M., Barber, G. P., Clawson, H., Coelho, A.*, et al.* (2011). The UCSC Genome Browser database: update 2011. Nucleic Acids Res. *39*, D876-D882.

Garro, A. J., Erlanger, B. F., and Beiser, S. M. (1968). Specificity in the reaction between anti-pyrimidine nucleoside antibodies and DNA. In Nucleic Acids in Immunology, O. Plescia, and W. Braun, eds. (Springer Berlin Heidelberg), pp. 47-57.

Huang, D. W., Sherman, B. T., and Lempicki, R. A. (2008). Systematic and integrative analysis of large gene lists using DAVID bioinformatics resources. Nat Protocols *4*, 44-57.

Huang, D. W., Sherman, B. T., and Lempicki, R. A. (2009). Bioinformatics enrichment tools: paths toward the comprehensive functional analysis of large gene lists. Nucleic Acids Res. *37*, 1-13.

Kashiwagi, K., Nimura, K., Ura, K., and Kaneda, Y. (2011). DNA methyltransferase 3b preferentially associates with condensed chromatin. Nucleic Acids Res. *39*, 874-888.

Kumaki, Y., Oda, M., and Okano, M. (2008). QUMA: quantification tool for methylation analysis. Nucleic Acids Res. *36*, W170-W175.

Li, H., and Durbin, R. (2009). Fast and accurate short read alignment with Burrows–Wheeler transform. Bioinformatics *25*, 1754-1760.

Maksimovic, J., Gordon, L., and Oshlack, A. (2012). SWAN: Subset-quantile Within Array Normalization for Illumina Infinium HumanMethylation450 BeadChips. Genome Biol. *13*, R44.

Putiri, E., Tiedemann, R., Thompson, J., Liu, C., Ho, T., Choi, J.-H., and Robertson, K. (2014). Distinct and overlapping control of 5-methylcytosine and 5-hydroxymethylcytosine by the TET proteins in human cancer cells. Genome Biol. *15*, R81.

Van Emburgh, B. O., and Robertson, K. D. (2011). Modulation of Dnmt3b function in vitro by interactions with Dnmt3L, Dnmt3a and Dnmt3b splice variants. Nucleic Acids Res. *39*, 4984-5002.

Widschwendter, M., Fiegl, H., Egle, D., Mueller-Holzner, E., Spizzo, G., Marth, C., Weisenberger, D. J., Campan, M., Young, J., Jacobs, I., and Laird, P. W. (2007). Epigenetic stem cell signature in cancer. Nat Genet *39*, 157-158.

Zang, C., Schones, D. E., Zeng, C., Cui, K., Zhao, K., and Peng, W. (2009). A clustering approach for identification of enriched domains from histone modification ChIP-Seq data. Bioinformatics *25*, 1952-1958.

Zimmermann, C., Guhl, E., and Graessmann, A. (1997). Mouse DNA methyltransferase (MTase) deletion mutants that retain the catalytic domain display neither de novo nor maintenance methylation activity in vivo. Biol Chem *378*, 393-405.